

Population pulsations and the dynamic Stark effect

Robert W. Boyd

Institute of Optics, University of Rochester, Rochester, New York 14627

Murray Sargent III

Optical Sciences Center, University of Arizona, Tucson, Arizona 85721

Received September 16, 1987; accepted October 5, 1987

We present a theoretical description of the interaction of optical waves due to the resonant nonlinear response of an atomic system. We emphasize how the resonant nature of the nonlinear coupling is modified by the shifting of the atomic energy levels as a consequence of the dynamic Stark effect and show the equivalent role played by population pulsations in determining the nature of the nonlinear coupling. A general formalism is developed to treat these effects and is explicitly applied to several examples of current interest, including single-beam saturation spectroscopy, pump-probe saturation spectroscopy, modulation spectroscopy, degenerate four-wave mixing for phase conjugation, and instabilities in the beam propagation through resonant media.

1. INTRODUCTION

This paper treats the subject of one or more weak waves interacting with a two-level medium subjected to a strong wave. Examples of these kinds of interaction include probe-saturator spectroscopy,¹⁻¹⁰ modulation spectroscopy,^{7,11-15} resonance fluorescence,¹⁶⁻¹⁹ phase conjugation by four-wave mixing,²⁰⁻²⁶ optical instabilities,²⁷⁻³² and the generation of squeezed states.³³⁻³⁵ There are two main approaches to these interactions: (1) the dressed-states method³⁶⁻³⁹ and (2) the bare-states or population-pulsation method.^{8,40,41} The former uses eigenstates of the coupled strong-wave/atom Hamiltonian, and the latter uses the unperturbed eigenstates. The approaches are equivalent, but each offers certain computational advantages and its own special insights. For example, it is easy to understand that the populations of unperturbed energy eigenstates pulsate at the beat frequency between two modes interacting with them, much as a square-law detector responds to the beat frequency between two waves incident upon it. On the other hand, it is also natural to envisage an atom interacting with a strong wave as a modified atom-field system whose energy eigenstates are fairly easily obtained. The weak fields then probe this atom-field system. This second approach is useful in demonstrating how the resonant structure of the nonlinear mixing process is modified by the presence of the intense field.

To concentrate on the basic phenomena, we consider only homogeneously broadened two-level media interacting with classical fields. Extensions to inhomogeneously broadened media, more levels, and quantized fields are given in the references. Section 2 introduces the dressed-states approach. Section 3 treats an arbitrarily intense single-mode field interacting with a two-level atom. This section introduces our population-matrix notation and derives the single-mode absorption coefficient. Section 4 uses the single-frequency polarization of Section 3 to calculate two important multimode generalizations of the single-mode case, namely, the degenerate-frequency cases of the probe-ab-

sorption coefficient and the coupled-mode equations for four-wave mixing. We find that the absorption experienced by the probe is substantially reduced below that experienced by a single wave of the same total intensity. This result can be understood as a consequence of the constructive scattering of the strong wave into the path of the probe wave, thereby reducing the absorption of the probe wave. Similarly we see that the coupling between the signal and conjugate waves in four-wave mixing can be understood in terms of the scattering of the pump off a nonlinear-response grating whose origin can be traced to population pulsations. Section 5 generalizes this single-frequency discussion to treat nondegenerate interactions that reveal the pulsations at the probe-saturator beat frequencies. Section 6 illustrates the nondegenerate absorption and reflection spectra predicted by the theory.

2. DRESSED-STATES APPROACH

In this section we see how the energy-level structure of a two-level atom is modified by the presence of a strong monochromatic, saturating laser field.³⁶ We use a particularly simple model that ignores damping effects and assumes that the time evolution of the system is governed by the semiclassical Hamiltonian

$$\mathcal{H} = \mathcal{H}_0 + \mathcal{V}(t). \quad (1)$$

Here \mathcal{H}_0 is the Hamiltonian of the unperturbed atom and $\mathcal{V}(t)$ is the electric-dipole interaction energy

$$\mathcal{V}(t) = erE(t), \quad (2)$$

where $-er$ is the atomic electric-dipole operator ($-e$ is the charge of the electron) and $E(t)$ is the laser electric field

$$E(t) = \frac{1}{2} \mathcal{E} e^{-i\omega t} + \text{c.c.} \quad (3)$$

We assume that the energy eigenstates of the unperturbed Hamiltonian are given by

$$\psi_j(\mathbf{r}, t) = u_j(\mathbf{r})\exp(-i\omega_j t) \quad j = a, b. \quad (4)$$

The requirement that each ψ_j satisfy the Schrödinger equation

$$i\hbar \frac{\partial \psi(\mathbf{r}, t)}{\partial t} = \mathcal{H}\psi(\mathbf{r}, t) \quad (5)$$

for \mathcal{H} equal to the atomic Hamiltonian \mathcal{H}_0 implies that the spatially varying part of the wave function must satisfy the equation

$$\mathcal{H}_0 u_j(\mathbf{r}) = \hbar\omega_j u_j(\mathbf{r}). \quad (6)$$

In the presence of the intense laser field, the wave function of the atom can be represented as a linear superposition of the two eigenstates as

$$\psi(\mathbf{r}, t) = C_a'(t)u_a(\mathbf{r})\exp(-i\omega_a t) + C_b'(t)u_b(\mathbf{r})\exp(-i\omega_b t), \quad (7)$$

where C_a' and C_b' denote the probability amplitudes that the atom is in the excited or ground state, respectively. We now require that this wave function obey the Schrödinger equation [Eq. (5)] with the Hamiltonian of Eq. (1). We assume that the atomic wave functions have definite parity so that the dipole-moment operator possesses only off-diagonal matrix elements. We then find that the nonvanishing matrix elements of the interaction energy are given in the rotating-wave approximation by

$$\mathcal{V}_{ab} = \mathcal{V}_{ba}^* = -\frac{1}{2}\mathcal{J}\mathcal{E}e^{-i\nu t}, \quad (8)$$

where $\mathcal{J} = \langle a|e^{-i\mathbf{r}}|b\rangle$. Because ν may differ somewhat from $\omega \equiv \omega_a - \omega_b$, it is convenient to write $\psi(\mathbf{r}, t)$ slightly differently from Eq. (7), namely, as

$$\begin{aligned} \psi(\mathbf{r}, t) = & C_a(t)\exp[-i(\omega_a - \delta/2)t]u_a(\mathbf{r}) + C_b(t) \\ & \times \exp[-i(\omega_b + \delta/2)t]u_b(\mathbf{r}), \end{aligned} \quad (9)$$

whose solution is in terms of sines and cosines. In particular if at time $t = 0$ the atom is in the lower state [$C_b(0) = 1$, $C_a(0) = 0$], then

$$C_b(t) = \cos(\Omega t/2), \quad (13)$$

which from Eq. (11) gives

$$C_a(t) = i \sin(\Omega t/2), \quad (14)$$

The probability that the system is in the lower level is $|C_b(t)|^2 = \cos^2(\Omega t/2) = (1 + \cos \Omega t)/2$, while $|C_a(t)|^2 = \sin^2(\Omega t/2) = (1 - \cos \Omega t)/2$. Hence the probability of being in the upper or lower state oscillates sinusoidally at the frequency $\Omega = \mathcal{J}\mathcal{E}_0/\hbar$, which is called the Rabi flopping frequency after Rabi,⁴² who studied a similar system (spin 1/2 magnetic dipole) in nuclear magnetic resonance.

To solve coupled equations (10) and (11) including a nonzero δ , we write them as the single matrix equation

$$\frac{d}{dt} \begin{bmatrix} C_a(t) \\ C_b(t) \end{bmatrix} = \frac{i}{2} \begin{bmatrix} -\delta & \Omega \\ \Omega & \delta \end{bmatrix} \begin{bmatrix} C_a(t) \\ C_b(t) \end{bmatrix}. \quad (15)$$

This is a vector equation of the form $d\mathbf{C}/dt = \mathbf{H}\mathbf{C}$, which has solutions of the form $e^{i\lambda t}$. Accordingly, substituting $\mathbf{C}(t) = \mathbf{C}(0)e^{i\lambda t}$ into Eq. (15), we seek values of λ that yield $\det(\mathbf{H} - i\lambda\mathbf{I}) = 0$. This latter equation gives the eigenvalues

$$\lambda = \pm \frac{1}{2} \sqrt{\delta^2 + \Omega^2} \equiv \pm \frac{\Omega'}{2}, \quad (16)$$

which lead to simple sinusoidal solutions of the form

$$\begin{aligned} C_a(t) &= C_a(0)\cos(\Omega't/2) + A \sin(\Omega't/2), \\ C_b(t) &= C_b(0)\cos(\Omega't/2) + B \sin(\Omega't/2). \end{aligned}$$

Substituting these values into Eqs. (10) and (11) and setting $t = 0$, we immediately find the constants A and B . Collecting the results in matrix form, we have the general solution

$$\begin{bmatrix} C_a(t) \\ C_b(t) \end{bmatrix} = \begin{bmatrix} \cos(\Omega't/2) - i\delta\Omega'^{-1} \sin(\Omega't/2) & i\Omega\Omega'^{-1} \sin(\Omega't/2) \\ i\Omega\Omega'^{-1} \sin(\Omega't/2) & \cos(\Omega't/2) + i\delta\Omega'^{-1} \sin(\Omega't/2) \end{bmatrix} \begin{bmatrix} C_a(0) \\ C_b(0) \end{bmatrix}. \quad (17)$$

where the frequency detuning is defined as $\delta = \omega - \nu$. This choice places the wave function in the rotating frame used in Bloch-vector discussions. Substituting this expansion for ψ into Eq. (5) and projecting onto the eigenfunctions u_a and u_b , we find that

$$\dot{C}_a = i/2(-\delta C_a + \Omega C_b), \quad (10)$$

$$\dot{C}_b = i/2(\delta C_b + \Omega C_a), \quad (11)$$

where $\Omega = \mathcal{J}\mathcal{E}/\hbar$ is assumed to be real for simplicity. These equations have the form of coupled differential equations with constant coefficients. If we do not include the terms $\pm\delta/2$ in the exponentials in Eq. (9), the resulting equations contain coefficients with an explicit time dependence and are harder to solve.

Before solving Eqs. (10) and (11) generally, we can quickly discover the basic physics by considering the case of exact resonance, for which $\delta = 0$. We can then differentiate Eq. (11) with respect to t and substitute Eq. (10) to find

$$\ddot{C}_b = \frac{1}{4}\Omega^2 C_b, \quad (12)$$

For simplicity, we consider the case for which at time $t = 0$ the atom is in the lower state, that is, $C_b(0) = 1$ and $C_a(0) = 0$. According to Eq. (17), the atomic wave function [Eq. (9)] then reduces to

$$\begin{aligned} \psi(\mathbf{r}, t) = & \frac{i\Omega}{\Omega'} \sin(\Omega't/2)\exp[-i(\omega_a - \delta/2)t]u_a(\mathbf{r}) \\ & + \left[\cos(\Omega't/2) + \frac{i\Omega}{\Omega'} \sin(\Omega't/2) \right] \\ & \times \exp[-i(\omega_b + \delta/2)t]u_b(\mathbf{r}). \end{aligned} \quad (18)$$

This form for the wave function shows that the probability for the atom to be in the upper or lower level oscillates periodically in time at the Rabi frequency Ω' . For the case of exact resonance ($\delta = 0$), the probability to be in the upper level oscillates between the values zero and unity, whereas for the case of a nonzero detuning the atom is never driven totally into its upper level. To obtain an understanding of the nature of the nonlinear-optical properties of a two-level atom, we should examine this behavior in the frequency

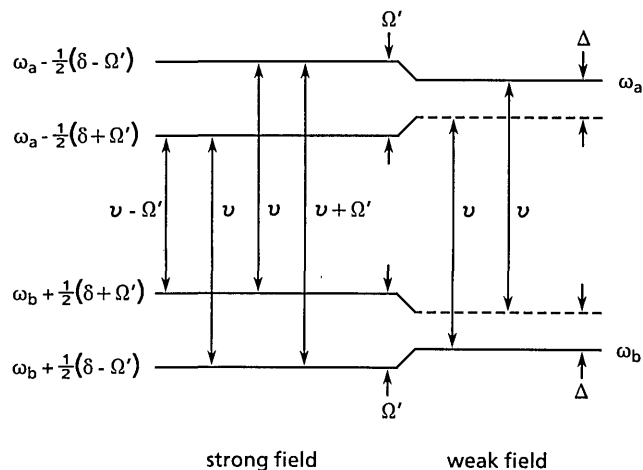


Fig. 1. Dressed levels of a two-level atom in the presence of strong laser field of frequency ν . These dressed levels lead to resonant response at frequencies ν and $\nu \pm \Omega'$. In the limit of a weak laser field, two of the dressed levels correspond to the virtual levels, shown as dashed lines.

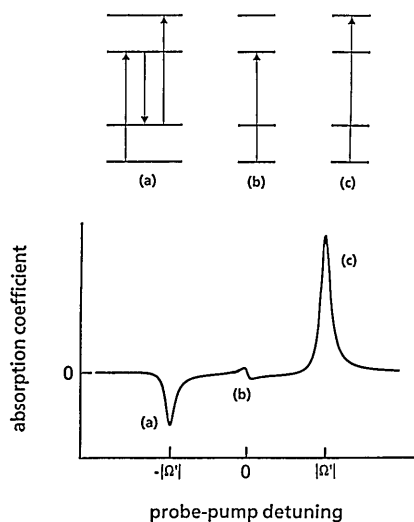


Fig. 2. Probe-absorption coefficient versus probe-saturator beat frequency Δ in the presence of a strong pump wave with $\delta T_2 = 5$, $\Omega' T_2 = 15$ for the case $T_2/T_1 = 2$. (a) The feature centered at frequency $\Delta = -\Omega'$ is due to the stimulated three-photon effect, (b) the feature centered at $\Delta = 0$ is due to the resonance induced at the laser frequency, and (c) the feature centered at frequency $\Delta = \Omega'$ is due to the atomic resonance shifted by the dynamic Stark effect. The energy-level diagrams at the top of the figure show the dressed-level transitions leading to each of these features.

domain rather than the time domain. Figure 1 shows the various frequency components present in the wave function of Eq. (18). Four frequencies are present. It is useful to think of these frequencies as the dressed levels of the atom, that is, of the atomic energy levels as modified by the presence of the intense laser field. We show below that the frequency differences between the levels shown in this diagram are in fact the resonance frequencies of the atom as modified by the presence of an intense laser field. We see that these resonances occur at the frequency ν of the laser field and at the Rabi-sideband frequencies $\nu \pm \Omega'$. Also shown in Fig. 1 are the locations of the dressed levels in the limit of a weak laser field. The dressed levels turn into the

unperturbed atomic levels and the levels, shown dashed, often referred to as virtual levels.

On the basis of the atomic-energy-level shifts predicted by the arguments just presented, it would be expected that the absorption spectrum experienced by a weak probe wave propagating through an atomic vapor in the presence of a strong laser beam would be dramatically modified. Such is in fact the case, as is illustrated in the example shown in Fig. 2. This probe-absorption spectrum was calculated using the density-matrix formalism described below and assumed the values $\delta T_2 = 5$, $\Omega' T_2 = 15$, and $T_2/T_1 = 2$. The maximum absorption does not occur at the weak-field atomic-resonance frequency but rather is shifted to the frequency $\nu + \Omega'$. The origin of this shift is illustrated on the accompanying dressed-level diagram. In addition to this resonance, two new spectral features are induced by the presence of the strong pump field. The region of negative absorption centered on the frequency $\nu - \Omega'$ is a consequence of the stimulated three-photon effect. As illustrated in the diagram at the top of Fig. 2, in this process the atom makes a transition from the lowest dressed level to the highest by the simultaneous absorption of two pump photons and the emission of a photon of energy $\nu - \Omega'$. The third resonance leads to the spectral feature centered at the pump-laser frequency having the shape of a dispersive profile. The existence of each of these features has been verified experimentally.^{13,14,43-45}

3. SINGLE-FREQUENCY POLARIZATION OF TWO-LEVEL MEDIA

In this section we derive an expression for the polarization of a two-level medium subject to a plane running-wave electric field

$$E(z, t) = \frac{1}{2} \mathcal{E}(z) e^{-i\nu t} + c.c. = \frac{1}{2} A(z) \exp[i(Kz - \nu t)] + c.c., \quad (19)$$

where ν is the oscillation frequency and K is the wave number, and where the complex field amplitude $A(z)$ is assumed to change little in an optical wavelength. This field induces in the medium a polarization of the similar form:

$$P(z, t) = \frac{1}{2} \mathcal{P}(z) e^{-i\nu t} + c.c. = \frac{1}{2} P(z) \exp[i(Kz - \nu t)] + c.c., \quad (20)$$

where the slowly varying complex polarization $p(z)$ is typically shifted in phase with respect to $A(z)$. We substitute these expressions into the driven-wave equation

$$\frac{\partial^2 E}{\partial z^2} + \epsilon \mu_0 \frac{\partial^2 E}{\partial t^2} = \mu_0 \frac{\partial^2 P}{\partial t^2}, \quad (21)$$

where ϵ is the permittivity index of the host material, and we make the slowly varying envelope approximation, that is, we neglect the second derivative of $A(z)$. This procedure yields the slowly varying amplitude form of Beer's law

$$dA/dz = i(K/2\epsilon)p = -\alpha A, \quad (22)$$

where the complex amplitude-absorption coefficient

$$\alpha = -i(K/2\epsilon)p/A = -i(K/2\epsilon)\mathcal{P}/\mathcal{E} \quad (23)$$

has been introduced. The corresponding equation for the dimensionless intensity $I = |pA/\hbar|^2 T_1 T_2$ is

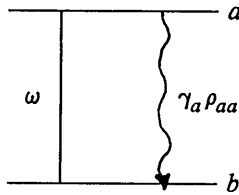


Fig. 3. Upper-to-ground-lower-level decay model.

$$\frac{dI}{dz} = -2 \operatorname{Re}(\alpha)I. \quad (24)$$

We have included the factor $\rho^2 T_1 T_2 / \hbar^2$ in the definition of I for reasons that become clear below in connection with Eq. (40). The problem of calculating the absorption coefficient experienced by the incident wave hence reduces to finding the polarization $\mathcal{P}(z)$ induced by $\mathcal{E}(z)$.

To do this we suppose that the medium consists of a collection of two-level systems with upper-to-ground-state decay as depicted in Fig. 3. The ruby-laser medium is approximated by this model, as are many media of interest in saturation spectroscopy and phase conjugation. For many laser media, both the upper and lower levels are excited by the incoherent pump process, and both experience decay. The equations of motion for the corresponding two-level density matrices differ somewhat from those relevant to Fig. 3, although the formulas for the steady-state polarizations are very similar.

We describe the two-level system shown in Fig. 3 in terms of a population matrix defined by

$$\rho(z, t) = N \rho_{\text{atom}}(z, t), \quad (25)$$

where $\rho_{\text{atom}}(z, t)$ is the density matrix describing one particular atom and where N is the total number of atoms per unit volume. $\rho(z, t)$ is called a population matrix because its diagonal elements give the population densities (rather than probabilities) of the levels. In terms of the population matrix, the polarization [Eq. (20)] is given by

$$P(z, t) = \rho_{ab}(z, t) + \text{c.c.} \quad (26)$$

As we shall see shortly [in Eq. (35)], ρ_{ab} varies as $\exp[i(Kz - \nu t)]$, so that we can combine Eqs. (20) and (26) to find

$$\mathcal{P}(z) = 2\rho e^{i\nu t} \rho_{ab}. \quad (27)$$

We must next find how $\rho_{ab}(z, t)$ evolves in time under the influence of the electric-dipole interaction energy. The component equations of motion for the population matrix $\rho(z, t)$ are given by⁸

$$\dot{\rho}_{ab} = -(i\omega + \gamma)\rho_{ab} + i\hbar^{-1}\mathcal{V}_{ab}(z, t)(\rho_{aa} - \rho_{bb}), \quad (28)$$

$$\dot{\rho}_{aa} = -\gamma_a \rho_{aa} - (i\hbar^{-1}\mathcal{V}_{ab}\rho_{ba} + \text{c.c.}), \quad (29)$$

$$\dot{\rho}_{bb} = +\gamma_a \rho_{aa} + (i\hbar^{-1}\mathcal{V}_{ab}\rho_{ba} + \text{c.c.}) = -\dot{\rho}_{aa}. \quad (30)$$

These equations are obtained from Schrödinger's equation. The damping terms involve the dipole dephasing rate γ , and the upper-level population-decay rate γ_a is added phenomenologically. The population equations of motion [Eqs. (29) and (30)] can next be combined into the single equation of motion for the population difference

$$D \equiv \rho_{aa} - \rho_{bb}, \quad (31)$$

namely,

$$\begin{aligned} \dot{D} &= -2\gamma_a D - D(i\hbar^{-1}\mathcal{V}_{ab}\rho_{ba} + \text{c.c.}) \\ &= -\gamma_a D - \gamma_a N - 2(i\hbar^{-1}\mathcal{V}_{ab}\rho_{ba} + \text{c.c.}). \end{aligned} \quad (32)$$

For the single-frequency field of Eq. (19), the perturbation energy \mathcal{V}_{ab} , in the rotating-wave approximation, is given by the expression

$$\mathcal{V}_{ab} = -\frac{1}{2}\rho A(z)\exp[i(Kz - \nu t)]. \quad (33)$$

Let us first examine the nature of the solution to these equations in the rate-equation approximation. We first note that Eq. (28) has the integral form

$$\rho_{ab}(z, t) = i \int_{-\infty}^t dt' \exp[-(i\omega + \gamma)(t - t')] \mathcal{V}_{ab}(z, t') D(z, t'). \quad (34)$$

The rate-equation approximation consists of assuming that the dipole-decay time $T_2 \equiv 1/\gamma$ is much smaller than times for which the population difference or the field envelope can change. For a monochromatic field, this approximation is essentially exact. We can then factor both the population difference and the field envelope outside the t' integration, perform the integral over exponentials [using Eq. (33) for \mathcal{V}_{ab}], and find that

$$\rho_{ab}(z, t) = -\frac{1}{2} i(\rho A/\hbar)\exp[i(Kz - \nu t)] \frac{D}{\gamma + i(\omega - \nu)}. \quad (35)$$

Substituting this expression into the population Eqs. (29) and (30), we find that the population difference obeys the rate equation

$$\dot{D} = -\gamma_a D - \gamma_a N - RD, \quad (36)$$

where the rate constant R is given by

$$R = \frac{1}{2} |\rho A/\hbar|^2 \gamma^{-1} \mathcal{L}(\omega - \nu) \quad (37)$$

and the dimensionless Lorentzian $\mathcal{L}(\omega - \nu)$ is given by

$$\mathcal{L}(\omega - \nu) = \frac{\gamma^2}{\gamma^2 + (\omega - \nu)^2}. \quad (38)$$

In steady state (i.e., for $\dot{D} = 0$), we find that the population difference is given by

$$D(z) = \frac{N(z)}{1 + I\mathcal{L}(\omega - \nu)}, \quad (39)$$

where the dimensionless intensity I is defined by

$$I = |\rho A/\hbar|^2 T_1 T_2, \quad (40)$$

where, for the level scheme of Fig. 3, $T_1 = 1/\gamma_a$. This dimensionless intensity is the intensity $c\epsilon|A|^2$ given in units of the saturation intensity

$$I_s = c\epsilon|\hbar/\rho|^2 / T_1 T_2. \quad (41)$$

For example, for $I = 1$ the population difference is reduced to one half of its unsaturated value.

Combining the expression for saturated population difference [Eq. (39)] with that for the off-diagonal population-matrix element [Eq. (35)], we find that ρ_{ab} is given by

$$\rho_{ab} = -i(\rho A/2\hbar)\exp[i(Kz - \nu t)] \frac{ND(\omega - \nu)}{1 + I\mathcal{L}(\omega - \nu)}, \quad (42)$$

where the complex Lorentzian denominator is defined through

$$\mathcal{D}(\omega - \nu) = \frac{1}{\gamma + i(\omega - \nu)}. \quad (43)$$

Using Eq. (27), we find the desired complex polarization

$$\mathcal{P}(z) = -i(\rho^2/\hbar) \frac{N\mathcal{D}(\omega - \nu)}{1 + I\mathcal{L}(\omega - \nu)} \mathcal{E}. \quad (44)$$

Substituting Eq. (44) into Eq. (23), we find the complex, nonlinear absorption coefficient

$$\alpha = \alpha_0 \frac{\gamma\mathcal{D}(\omega - \nu)}{1 + I\mathcal{L}(\omega - \nu)}, \quad (45)$$

where the unsaturated ($I = 0$), line-center ($\nu = \omega$) absorption coefficient

$$\alpha_0 = K \frac{\rho^2 N}{2\epsilon\hbar\gamma}. \quad (46)$$

Combining Eqs. (24) and (45), we obtain

$$\frac{dI}{dz} = \frac{2\alpha_0\mathcal{L}}{-1 + I\mathcal{L}} I, \quad (47)$$

where $\mathcal{L} \equiv \mathcal{L}(\omega - \nu)$. For small $I\mathcal{L}$, I decays exponentially to 0. For large $I\mathcal{L}$, I decays linearly in z with the slope $-2\alpha_0$. For a two-level medium with pumping, the number N of atoms per volume in Eq. (46) is replaced by the difference between the lower- and upper-level unsaturated populations. Hence, for a gain medium, $\alpha_0 < 0$, and I grows exponentially at first and then approaches a linear growth rate.

The real part of the absorption coefficient in Eq. (45) can be expressed explicitly as

$$\text{Re}(\alpha) = \alpha_0 \frac{\gamma^2}{\gamma^2(1 + I) + (\omega - \nu)^2}, \quad (48)$$

which has the form of a power-broadened Lorentzian. Note that although the width of the Lorentzian in Eq. (48) increases as the intensity increases, the value of the absorption for any given tuning decreases.

4. DEGENERATE PROBE ABSORPTION AND DEGENERATE FOUR-WAVE MIXING

We can use the single-frequency polarization of Eq. (44) to calculate the absorption coefficient experienced by a weak probe wave in the presence of a strong wave at the same frequency, as depicted in Fig. 4(a). We have already solved the dynamics of this problem in Section 3; we need only generalize the way in which we project the total polarization onto the pump and probe modes. We see below that the probe absorption is reduced substantially below that given by Eq. (45) for a single wave. Similarly we can derive the degenerate-frequency-coupled amplitude equations that govern the propagation of two weak waves, the so-called signal and conjugate waves, for either three- or four-wave mixing [Figs. 4(b) and 4(c)].

Suppose that the electric field consists of a strong wave and a weak wave having the same frequency but different propagation directions. We want to calculate the absorption coefficient for the weak wave. To do this, we replace

the electric-field-amplitude factor $A(z)e^{iKz}$ in Eq. (19) by the more general function of \mathbf{r} :

$$\begin{aligned} E(\mathbf{r}, t) &= \frac{1}{2}\mathcal{E}(\mathbf{r})e^{-i\nu t} + \text{c.c.} \\ &= \frac{1}{2}[\mathcal{E}_2(\mathbf{r}) + \epsilon(\mathbf{r})]e^{-i\nu t} + \text{c.c.} \\ &= \frac{1}{2}[A_2(\mathbf{r})U_2(\mathbf{r}) + \epsilon(\mathbf{r})]e^{-i\nu t} + \text{c.c.}, \end{aligned} \quad (49)$$

where $\mathcal{E}_2(\mathbf{r})$ is the complex amplitude of the arbitrarily strong pump (or saturator) wave, $A_2(\mathbf{r})$ is its slowly varying amplitude, $U_2(\mathbf{r})$ is its spatial distribution function [$\exp(i\mathbf{K}_2 \cdot \mathbf{r})$ for a running wave], and $\epsilon(\mathbf{r})$ is the field amplitude of the weak wave. The polarization [Eq. (44)] then takes the form

$$\mathcal{P}[\mathcal{E}(\mathbf{r}), \mathcal{E}^*(\mathbf{r})] = i \frac{(\rho^2/\hbar)N\mathcal{D}\mathcal{E}}{1 + \frac{\mathcal{E}\mathcal{E}^*\mathcal{L}}{\mathcal{E}_s^2}}, \quad (50)$$

where $\mathcal{E}_s^2 = (\hbar/\rho)^2/T_1T_2$. To first order in ϵ and ϵ^* , the total polarization amplitude [Eq. (50)] is given by

$$\begin{aligned} \mathcal{P}(\mathcal{E}_2 + \epsilon, \mathcal{E}_2^* + \epsilon^*) &= i \frac{(\rho^2/\hbar)N\mathcal{D}\mathcal{E}}{(1 + I_2\mathcal{L}) \left[1 + \frac{(\epsilon\mathcal{E}_2^* + \epsilon^*\mathcal{E}_2)\mathcal{L}}{\mathcal{E}_s^2(1 + I_2\mathcal{L})} \right]} \\ &\approx i \frac{(\rho^2/\hbar)N\mathcal{D}\mathcal{E}}{1 + I_2\mathcal{L}} \\ &\quad \times \left[1 - \frac{(\epsilon\mathcal{E}_2^* + \epsilon^*\mathcal{E}_2)\mathcal{L}}{\mathcal{E}_s^2(1 + I_2\mathcal{L})} \right], \end{aligned} \quad (51)$$

where $I_2 = (\rho A_2/\hbar)^2 T_1 T_2$. The term containing the weak-wave/strong-wave interference factor $(\epsilon\mathcal{E}_2^* + \epsilon^*\mathcal{E}_2)$ represents the dc limit of the population-pulsation factor. As we see below, it leads to scattering of the strong wave into the weak waves. In particular, suppose that $\epsilon(\mathbf{r})$ is the field

$$\epsilon(\mathbf{r}) = A_1 \exp(i\mathbf{K}_1 \cdot \mathbf{r}), \quad (52)$$

where A_1 is assumed to vary little in a wavelength. We choose the z axis such that $\mathbf{K}_1 \cdot \mathbf{r} = K_1 z$. The slowly varying

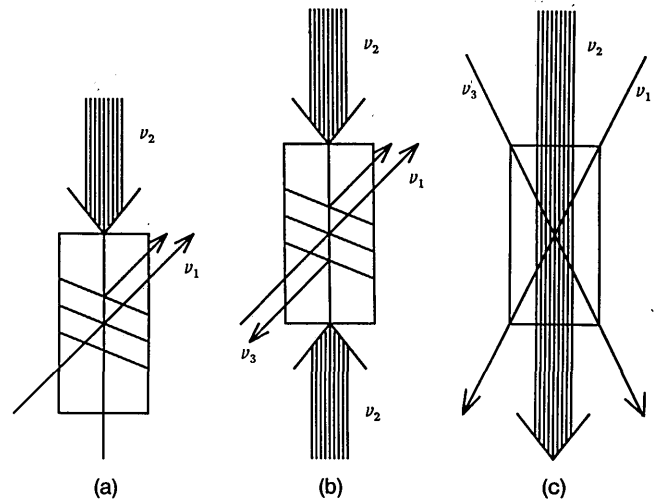


Fig. 4. (a) Measurement of the absorption experienced by a probe wave in a medium subjected to a strong wave. (b) Three-wave mixing. (c) Four-wave mixing.

polarization component $P_1(z)$ that contributes to a Beer law [Eqs. (22) and (23)] for $A_1(z)$ is given by that part of \mathcal{P} that varies spatially as $\exp(i\mathbf{K}_1 \cdot \mathbf{r})$, that is, by the projection

$$P_1(z) = \frac{K_1}{2n\pi} \int_0^{2n\pi/K_1} d\zeta \exp[-iK_1(z + \zeta)] \mathcal{P}(\mathbf{r}), \quad (53)$$

where \mathcal{P} is given by Eq. (51) and n is a sufficiently small integer that $\mathcal{E}_1(z)$ varies little in the distance $2n\pi/K_1$. In carrying out this projection, we suppose the angle between \mathbf{K}_1 and \mathbf{K}_2 is sufficiently large that the contribution from ϵ^* is negligible (ϵ^* leads primarily to three- and four-wave mixing, as discussed below). We thus obtain

$$\begin{aligned} P_1(z) &= \frac{\rho^2 N \mathcal{D}}{1 + I_2 \mathcal{L}} \left(1 - \frac{I_2 \mathcal{L}}{1 + I_2 \mathcal{L}} \right) A_1 \\ &= \frac{\rho^2 N \mathcal{D}}{(1 + I_2 \mathcal{L})^2} A_1. \end{aligned} \quad (54)$$

Substituting this polarization component into Beer's law [Eqs. (4) and (5)], we find for the absorption coefficient

$$\alpha_1 = \alpha_0 \gamma \mathcal{D} / (1 + I_2 \mathcal{L})^2. \quad (55)$$

Comparing this equation with the single-mode absorption coefficient of Eq. (45), we see that the probe-absorption coefficient is reduced by an additional factor of $1/(1 + I_2 \mathcal{L})$. This reduction can be understood in terms of the grating picture that is often used to describe four-wave mixing processes. Specifically, the probe and saturator waves interfere to form a fringe pattern in the two-level nonlinear medium. The fringe induces a grating in the population difference, which scatters the saturator wave into the oncoming path of the probe wave. This scattering is represented by the $-I_2 \mathcal{L}/(1 + I_2 \mathcal{L})$ factor in the first line of Eq. (54). For this degenerate-frequency case, the scattering is constructive, thereby reducing the probe's absorption.

To see why the scattering is constructive, we note that when the two fields interfere constructively, they create a slightly larger total field that saturates the medium slightly more than the average. In contrast, when the fields interfere destructively, they saturate the medium less. The projection [Eq. (53)] of the total polarization onto the probe mode samples the constructive (more saturated) portion more than the destructive (less saturated) case. Hence the projection selects a more-than-average saturation absorption for the probe, which implies reduced probe absorption.

To treat degenerate-frequency three- and four-wave mixing, we take $\epsilon(\mathbf{r})$ as the sum of two weak fields

$$\epsilon(\mathbf{r}) = \mathcal{E}_1 + \mathcal{E}_3 = A_1 \exp(i\mathbf{K}_1 \cdot \mathbf{r}) + A_3 \exp(i\mathbf{K}_3 \cdot \mathbf{r}), \quad (56)$$

where A_1 and A_3 vary little in a wavelength along their respective propagation directions. More-general wave fronts can be represented by a sum over such amplitudes. Two kinds of pump wave that are of interest are the traveling pump wave $U_2(\mathbf{r}) = \exp(i\mathbf{K}_2 \cdot \mathbf{r})$, which gives rise to three-wave mixing, and the standing pump wave $U_2(\mathbf{r}) = \cos(\mathbf{K}_2 \cdot \mathbf{r})$, which gives rise to four-wave mixing.

For the three-wave case of Fig. 4(b), we substitute Eqs. (56) and (51) into the probe-polarization integral [Eq. (53)] to find

$$P_1(z) = \frac{\rho^2 N \mathcal{D}}{(1 + I_2 \mathcal{L})^2} (A_1 - A_3^* I_2 \mathcal{L} e^{i\Delta K z}), \quad (57)$$

where we have introduced the phase-mismatch factor $\Delta K z = (\mathbf{K}_1 - 2\mathbf{K}_2 + \mathbf{K}_3) \cdot \mathbf{r}$. Note that the entire A_3^* contribution comes from the scattering term in Eq. (51), which is the result of the dc limit of population pulsations. A similar expression is obtained for $P_3(z)$. Substituting these polarization components into Beer's law in Eq. (22), we find the coupled-amplitude equations

$$\frac{dA_1}{dz} = -\alpha_1 A_1 + \chi_1 A_3^* \exp(2i\Delta K z), \quad (58)$$

$$\frac{dA_3^*}{dz} = -\alpha_3^* A_3^* + \chi_3^* A_1 \exp(-2i\Delta K z), \quad (59)$$

where the absorption coefficient α_1 is given by Eq. (55), the coupling coefficient χ_1 is given by

$$\chi_1 = -\alpha_0 \gamma \mathcal{D} I_2 \mathcal{L} / (1 + I_2 \mathcal{L})^2, \quad (60)$$

and the phase-mismatch factor ΔK is given by

$$\Delta K = |2\mathbf{K}_2 - \mathbf{K}_1 - \mathbf{K}_3|. \quad (61)$$

For this degenerate-frequency case, α_3 and χ_3 are also given by Eqs. (55) and (60), respectively.

For the four-wave case of Fig. 4(c), the squared saturation denominator in Eq. (51) has spatial holes. Unless \mathbf{K}_1 and \mathbf{K}_2 are nearly parallel, the projection in z of Eq. (53) averages over these holes. Including this average and changing the variable of integration from $2K_1 \zeta$ to θ , we have

$$\begin{aligned} P_1(z) &= i \rho^2 \hbar^{-1} N \mathcal{D} \\ &\times \frac{1}{2\pi} \int_0^{2\pi} d\theta \left[\frac{A_1}{(a + b \cos \theta)^2} - A_3^* b \frac{1 + \cos \theta}{(a + b \cos \theta)^2} \right], \end{aligned} \quad (62)$$

where $b = 2I_2 \mathcal{L}$ and $a = 1 + b$. Simplifying, we obtain

$$\begin{aligned} P_1 &= -i \rho^2 \hbar^{-1} N \mathcal{D} \frac{\partial}{\partial a} \frac{1}{2\pi} \int_0^{2\pi} d\theta \left[\frac{A_1 + A_3^*(a - b)}{a + b \cos \theta} - A_3^* \right] \\ &= i \frac{\rho^2 N \mathcal{D}}{\hbar(1 + 2b)^{3/2}} [A_1(1 + b) - A_3^* b]. \end{aligned} \quad (63)$$

We again substitute this polarization into Beer's law and find a coupled amplitude equation of the form of Eq. (58) with coefficients

$$\alpha_1 = \frac{\alpha_0 \gamma \mathcal{D} (1 + 2I_2 \mathcal{L})}{(1 + 4I_2 \mathcal{L})^{3/2}}, \quad (64)$$

$$\chi_1 = \frac{2\alpha_0 \gamma \mathcal{D} I_2 \mathcal{L}}{(1 + 4I_2 \mathcal{L})^{3/2}} \quad (65)$$

but with ΔK identically zero. The coupled-mode equation [Eq. (59)] for A_3 has the same coefficients as in Eqs. (64) and (65) for this degenerate-frequency case, and again no phase mismatch occurs.

5. NONDEGENERATE-FREQUENCY ABSORPTION AND COUPLING COEFFICIENTS

In Sections 3 and 4 we treated probe absorption and three- and four-wave mixing in the limit in which all the applied fields were at the same frequency. To treat the nondegenerate-frequency case, we have to consider the dynamics of the population-matrix equations of motion [Eqs. (9) and (13)] for multiple frequencies. This section carries out that derivation and shows explicitly the role of population pulsations in determining the form of the nonlinear coupling. Our results reduce to those of Sections 3 and 4 in the limit of degenerate frequencies. The present derivation hence justifies the statements made regarding the role of population pulsations in the dc limit in determining the form of the nonlinear coupling for the degenerate case.

We take the electric field to have the form

$$\begin{aligned} E(\mathbf{r}, t) &= \frac{1}{2} \sum_n \mathcal{E}_n(\mathbf{r}) \exp(-i\nu_n t) + \text{c.c.} \\ &= \frac{1}{2} \sum_n A_n(\mathbf{r}) \exp[i(\mathbf{K}_n \cdot \mathbf{r} - \nu_n t)] + \text{c.c.} \end{aligned} \quad (66)$$

for $n = 1, 2$, and 3 , where the mode amplitudes $A_n(\mathbf{r})$ are in general complex and \mathbf{K}_n are the wave-propagation vectors. As in Section 4, A_2 is the amplitude of the arbitrarily intense field. The field [Eq. (66)] induces the polarization

$$P(\mathbf{r}, t) = \frac{1}{2} \sum_n P_n(\mathbf{r}) \exp[i(\mathbf{K}_n \cdot \mathbf{r} - \nu_n t)] + \text{c.c.} \quad (67)$$

for $n = 1, 2$, and 3 , where $P_n(\mathbf{r})$ is a complex polarization amplitude that can be used to calculate refractive index and absorption and gain characteristics for the probe and saturator waves. We are interested only in the components of $P(\mathbf{r}, t)$ given by Eq. (67), although in general the polarization has other components. For example, strong-wave interactions involving the ν_1 and ν_2 fields induce components not only at the frequencies ν_1 and ν_2 but also at $\nu_2 \pm k(\nu_2 - \nu_1)$, where k is any integer. To project the components $P_n(\mathbf{r})$ out of $P(\mathbf{r}, t)$, we can use the mode factors $\exp(i\mathbf{K}_n \cdot \mathbf{r})$, as in Eq. (53) above, provided that they differ sufficiently from one another over the relevant interaction distances. For copropagating (or nearly copropagating) waves, these mode functions do not vary sufficiently rapidly, and one must separate the components by their temporal differences, for example, by heterodyne techniques.

The problem hence reduces to determining the slowly varying complex polarization $P_1(\mathbf{r})$ driving the probe wave, from which the absorption coefficient is determined from an equation formally identical to Eq. (22) with a subscript 1 on A and α , and with p replaced by P_1 . One might (incorrectly) guess that the probe-absorption coefficient α_1 is simply a Lorentzian line-shape function for the probe frequency multiplied by the population difference calculated in the presence of the saturator wave. However, as in Eq. (54), an additional contribution enters as a result of population pulsations. Specifically, the medium responds to the superposition of the modes to give pulsations in the population difference at the beat frequency $\Delta = \nu_2 - \nu_1$. Since we assume that the probe is sufficiently weak that it cannot

saturate the medium, the pulsations occur only at $\pm\Delta$, as we demonstrate explicitly below. These pulsations act as modulators (or as Raman shifters), putting sidebands onto the medium's response to the strong ν_2 wave. One of these sidebands falls precisely at ν_1 , yielding a contribution to the probe-absorption coefficient. The other sideband leads to a response at the conjugate frequency $\nu_3 = \nu_2 + (\nu_2 - \nu_1)$.

The interaction-energy matrix element \mathcal{V}_{ab} appropriate to the field of Eq. (66) is given in the rotating-wave approximation by

$$\mathcal{V}_{ab} = -\frac{\mathcal{P}}{2\hbar} \sum_n \mathcal{E}_n(\mathbf{r}) \exp(-i\nu_n t). \quad (68)$$

To determine the response of the medium to this multimode field, we express both the polarization component ρ_{ab} and the population difference D as Fourier series:

$$\begin{aligned} \rho_{ab} &= N \exp[i(\mathbf{K}_1 \cdot \mathbf{r} - \nu_1 t)] \\ &\times \sum_{m=-\infty}^{\infty} p_{m+1} \exp[im[(\mathbf{K}_2 - \mathbf{K}_1) \cdot \mathbf{r} - \Delta t]] \end{aligned} \quad (69)$$

and

$$\begin{aligned} D(\mathbf{r}, t) &\equiv \rho_{aa}(\mathbf{r}, t) - \rho_{bb}(\mathbf{r}, t) \\ &= N \sum_{k=-\infty}^{\infty} d_k \exp[-ik[(\mathbf{K}_2 - \mathbf{K}_1) \cdot \mathbf{r} - \Delta t]]. \end{aligned} \quad (70)$$

We substitute these expansions into the population-matrix equations of motion [Eqs. (28)–(32)] and identify coefficients of common exponential frequency factors. We consider the general three-mode case but suppose that \mathcal{E}_1 and \mathcal{E}_3 are not sufficiently strong to saturate the medium. In this approximation only p_1, p_2 , and p_3 occur in the polarization expansion [Eq. (69)], and only d_0 and $d_{\pm 1}$ appear in the population-difference expansion [Eq. (70)]. The origin of this simplification can be understood by considering the number of times that each frequency component acts (in the sense of a perturbation expansion) in determining the response of the medium. After some arbitrary number of \mathcal{E}_2 interactions, the ν_1 field acts to give the products $E_1 \mathcal{E}_2^*$ and $\mathcal{E}_1^* \mathcal{E}_2$, which create the pulsations $d_{\pm 1}$. From then on only \mathcal{E}_2 can act, since a weak probe field may act only once. We hence obtain polarization sidebands of ν_2 at frequencies ν_1 and ν_3 , which subsequently combine with ν_2 to give only the $d_{\pm 1}$ population components.

We first calculate the amplitude p_2 in the presence of the saturator wave only, that is, we assume that only \mathcal{E}_2 is nonzero in Eq. (68). We find by substituting Eqs. (68)–(70) into Eq. (28) and equating terms that oscillate as $\exp(-i\nu_2 t)$ that

$$-i\nu_2 p_2 = -(i\omega + \gamma)p_2 - i(\mathcal{P}\mathcal{E}_2/2\hbar)d_0$$

and hence that

$$p_2 = -i(\mathcal{P}/2\hbar)\mathcal{E}_2\mathcal{D}_2 d_0, \quad (71)$$

where we have defined the complex denominator

$$\mathcal{D}_n = 1/[\gamma + i(\omega - \nu_n)]. \quad (72)$$

Equation (71) is simply an alternative way of writing the single-mode density-matrix element of Eq. (35).

We next calculate p_1 for the probe wave in an analogous manner. We find that

$$-i\nu_1 p_1 = -(i\omega + \gamma)p_1 - i(\rho/2\hbar)[\mathcal{E}_1 d_0 + \mathcal{E}_2 d_1],$$

giving

$$p_1 = -i(\rho/2\hbar)\mathcal{D}_1[\mathcal{E}_1 d_0 + \mathcal{E}_2 d_1]. \quad (73)$$

The term $\mathcal{E}_2 d_1$ leads to the scattering of \mathcal{E}_2 into the \mathcal{E}_1 mode by means of the population-pulsation component d_1 . Similarly, the component p_3 has the value

$$p_3 = -i(\rho/2\hbar)\mathcal{D}_3(\mathcal{E}_3 d_0 + \mathcal{E}_2 d_{-1}). \quad (74)$$

p_0 remains zero when only d_0 and $d_{\pm 1}$ are nonzero since it is proportional to $\mathcal{E}_1 d_1$, involving the product of at least two weak-field amplitudes (\mathcal{E}_1 's), while p_j for $j > 3$ vanishes since d_k for $k < 0$ would be involved.

We next calculate the Fourier components of the population difference. We first consider the dc component $d_0 = n_{a0} - n_{b0}$ as saturated by the pump wave \mathcal{E}_2 alone. Substituting Eq. (70) into Eq. (32) and equating the sum of the dc coefficients to zero, we obtain

$$0 = -\gamma_a d_0 - \gamma_a - (2\gamma)^{-1} |\rho \mathcal{E}_2 / \hbar|^2 \mathcal{L}_2 d_0. \quad (75)$$

Here the dimensionless Lorentzian of Eq. (38) is abbreviated as

$$\mathcal{L}_n = \gamma^2 / [\gamma^2 + (\omega - \nu_n)^2]. \quad (76)$$

The \mathcal{E}_1 contributions are ignored, since we have assumed that \mathcal{E}_1 does not saturate. Solving Eq. (75) for d_0 , we find that

$$\begin{aligned} d_0 &= -1 - I_2 \mathcal{L}_2 d_0 \\ &= -1 / (1 + I_2 \mathcal{L}_2). \end{aligned} \quad (77)$$

This result agrees with that of Eq. (39) for the population difference for the single-mode case.

We next calculate the coefficient d_1 . Substituting Eq. (70) into Eq. (32) and equating the sum of the coefficients of $e^{i\Delta t}$ to zero, we obtain

$$i\Delta d_1 = -\gamma_a d_1 + i(\rho/2\hbar)(\mathcal{E}_1 p_2^* + \mathcal{E}_2 p_3^* - \mathcal{E}_2^* p_1).$$

We now substitute Eqs. (71), (73), and (74) into this expression to obtain amplitude d_1 of the fundamental frequency of population pulsations as

$$d_1 = - \frac{(\rho/\hbar)^2 T_1 T_2 \mathcal{F}(\Delta) \frac{\gamma}{2} [\mathcal{E}_1 \mathcal{E}_2^* (\mathcal{D}_1 + \mathcal{D}_2^*) + \mathcal{E}_2 \mathcal{E}_3^* (\mathcal{D}_2 + \mathcal{D}_3^*)]}{1 + I_2 \mathcal{F}(\Delta) \frac{\gamma}{2} (\mathcal{D}_1 + \mathcal{D}_3^*)} d_0, \quad (78)$$

where we have introduced the dimensionless complex population-pulsation factor

$$\mathcal{F}(\Delta) = \frac{\gamma_a}{\gamma_a + i\Delta}. \quad (79)$$

This factor approaches unity as $\Delta \rightarrow 0$. Analogously, we find that the coefficient d_{-1} is given simply by $d_{-1} = d_1^*$.

Our calculation is self-consistent, since only d_0 , $d_{\pm 1}$ can obtain nonzero values from p_1 , p_2 , p_3 , and vice versa. Com-

binning the pulsation component [Eq. (78)] with the polarization component [Eq. (73)], setting $\mathcal{P}_1 = 2\rho N p_1$, and using Eqs. (53) and (23), we find that the amplitudes A_1 and A_3 obey the coupled-amplitude equation [Eqs. (58) and (59)] with the nondegenerate complex absorption coefficient

$$\begin{aligned} \alpha_1 &= \frac{\alpha_0 \gamma \mathcal{D}_1}{1 + I_2 \mathcal{L}_2} \left[1 - \frac{I_2 \mathcal{F}(\Delta) \frac{\gamma}{2} (\mathcal{D}_1 + \mathcal{D}_2^*)}{1 + I_2 \mathcal{F}(\Delta) \frac{\gamma}{2} (\mathcal{D}_1 + \mathcal{D}_3^*)} \right] \\ &= \alpha_{\text{inc}} + \alpha_{\text{coh}} \end{aligned} \quad (80)$$

and the complex coupling coefficient

$$\chi_1 = - \frac{\alpha_0 \gamma \mathcal{D}_1}{1 + I_2 \mathcal{L}_2} \frac{I_2 \mathcal{F}(\Delta) \frac{\gamma}{2} (\mathcal{D}_2 + \mathcal{D}_3^*)}{1 + I_2 \mathcal{F}(\Delta) \frac{\gamma}{2} (\mathcal{D}_1 + \mathcal{D}_3^*)}. \quad (81)$$

α_3 and χ_3 are given by similar equations obtained by interchanging the subscripts 1 and 3 and replacing Δ by $-\Delta$. Note that in the degenerate-frequency case ($\nu_1 = \nu_2 = \nu_3$), Eqs. (80) and (81) reduce to Eqs. (55) and (60), as they should.

The absorption coefficient consists of two contributions. One contribution results simply from the reduction of the population difference that is due to the presence of the ν_2 wave. This contribution leads to the 1 inside the square brackets and is called the incoherent contribution α_{inc} to α_1 . The second contribution involves the interference between \mathcal{E}_1 and \mathcal{E}_2 and hence depends on the factor $\mathcal{F}(\Delta)$ and is called the coherent contribution. It leads to the scattering of the saturator wave off the grating induced by the interference between the probe and saturator fields. In this terminology, the coupling coefficient of Eq. (81) is a coherent contribution, since it also results from the population-pulsation coefficient d_1 .

It is instructive to interpret the incoherent and coherent contributions in terms of the number of electric-dipole interactions. By restricting the intensity of the probe to nonsaturating values, we have obtained an expression valid for arbitrarily large values of the saturator intensity I_2 . The saturation denominator $1/(1 + I_2 \mathcal{L}_2)$ appearing in Eq. (80) expands to $1 - I_2 \mathcal{L}_2$ in the third-order approximation ($\mathcal{E}_1 \mathcal{E}_2 \mathcal{E}_2^*$ is involved). For much of saturation spectroscopy this value is inadequate, for I_2 is typically as large as unity or larger, and the geometric series fails to converge for any order! Hence we interpret Eq. (80) in a nonperturbative

fashion as follows: The saturator interacts with the unsaturated population difference N an effective number of times giving the summed series saturation factor $1/(1 + I_2 \mathcal{L}_2)$. Given an effective dc-saturated population difference $N/(1 + I_2 \mathcal{L}_2)$, the probe then interacts, producing a polarization at the probe frequency. This yields the incoherent contribution and in addition gives the start of $\mathcal{F}(\Delta) \mathcal{D}_1$ term in Eq. (80). For the latter, the saturator in turn interacts with the probe polarization to yield a population pulsation. Alterna-

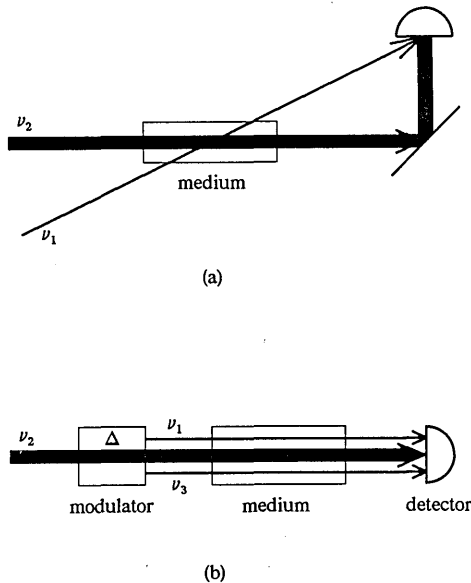


Fig. 5. Beat-frequency saturation spectroscopy configurations. (a) The beat-frequency signal at frequency $\Delta = \nu_2 - \nu_1$ resulting from the superposition of the probe and saturator waves is studied as a function of Δ . (b) The large intensity beam at frequency ν_2 passes through a modulator, producing two sidebands at the frequencies $\nu_1 = \nu_2 - \Delta$ and $\nu_3 = \nu_2 + \Delta$. The beat-frequency signal is studied as in (a).

tively to this probe interaction, the saturator interacts with the effective dc-saturated population difference to generate a polarization at the frequency ν_2 [giving the \mathcal{D}_2^* term in Eq. (80) without its denominator], followed by a probe interaction, a sequence also yielding a population pulsation. The saturator then interacts an additional amount represented by the denominator $1/[1 + I_2\mathcal{F}(\Delta) \dots]$ in Eq. (80) and corresponding to successive generations of probe polarizations (at ν_3 and ν_1 , i.e., at $\nu_2 \pm \Delta$) and population pulsations at Δ . These sequences give the scattering of the saturator into the probe wave, i.e., the coherent $\mathcal{F}(\Delta)$ term of Eq. (80). For a saturating probe, higher-order population pulsations (at $n\Delta$, $n > 1$) occur, forcing one to use the more general continued fraction. This truncates ultimately, owing to the finite bandwidth of the medium. For small Δ , a saturating probe can generate a substantial number of higher-order pulsations.

An interesting property of α_1 is that the integrated area under the curve $\alpha_1(\Delta)$ is independent of the coherent contribution α_{coh} . Whatever decrease in absorption results because of population pulsations for one value of Δ must be compensated for by increased absorption at some other values of Δ . The population pulsations hence merely redistribute the absorption as a function of Δ and do not modify the integrated absorption of the medium. To demonstrate this fact, we note that Eq. (80) interpreted as a function of Δ has no poles in the lower half-plane. Therefore the integral

$$\int_{-\infty}^{\infty} d\Delta \alpha_{\text{coh}}(\Delta) \quad (82)$$

must vanish. For the same reason, the integral of χ_1 vanishes. However, it can be shown that the result in expression (82) is no longer valid for the case of probe intensities sufficiently large to lead to saturation of the medium.

Before examining Eq. (80) in various special cases, we extend the treatment somewhat to include two experimental configurations (Fig. 5). In both cases the probe-saturator beat-frequency intensity is studied, and a heterodyne advantage is obtained in the signal-to-noise ratio. For the two-wave case of Fig. 5(a), the atom-field interaction is described as above. For the configuration of Fig. 5(b) the saturator wave is weakly modulated, imposing sidebands at frequencies ν_1 and ν_3 , which act as probes. The absorption coefficient for this case is similar to that for Fig. 5(a) but includes the effects of population pulsations generated by both the $\mathcal{E}_1\mathcal{E}_2^*$ and $\mathcal{E}_2\mathcal{E}_3^*$ interactions. Furthermore, the relative phase between the three fields is important. If at some time all three modes are in phase with one another, then the two population pulsation sources add. This case is called the amplified-modulation (AM) case. If the phases of the saturator and one sideband are equal and differ from the phase of the other sideband by π , the two population pulsations cancel out, giving a constant envelope in time. This case is called the frequency-modulated (FM) case. Both of these limiting cases have attracted substantial attention. The AM case has been used to measure T_1 for cases when $T_1 \gg T_2$.^{13,14} The FM case has been used by Bjorklund¹¹ and Drewer *et al.*,¹² who use the fact that the medium may modify the phase and amplitude relationships of an FM wave, thereby producing an easily detected AM component. In addition to spectroscopy, the problem is important in phase conjugation, laser instabilities, and cavity stabilization.

For simplicity we assume that \mathcal{E}_2 is real and take \mathcal{E}_3^* to be zero (the single-sideband case), equal to \mathcal{E}_1 (the AM case), or equal to $-\mathcal{E}_1$ (the FM case). In general the product $\mathcal{E}_2^2\mathcal{E}_3^*$ may not be phase matched to $\exp(i\mathbf{K}_1 \cdot \mathbf{r})$, so that $\Delta\mathbf{K}$ in coupled-mode equations (58) and (59) is nonzero. Such a mismatch reduces the effectiveness of the coupling term. For a sufficiently large angle between \mathbf{K}_1 and \mathbf{K}_2 , the coupling terms in Eqs. (58) and (59) can be dropped altogether.

For the case for central saturator tuning ($\nu_2 = \omega$), Eq. (58) leads to a simple physical interpretation. Since in this case $\mathcal{D}_3^* = \mathcal{D}_1$, $\mathcal{D}_2 = 1/\gamma$, and $\Delta\mathbf{K}$ vanishes identically, the spatial variation of the weak part of the field $\mathcal{E}_1 \exp(-i\nu_1 t) + \mathcal{E}_3 \exp(-i\nu_3 t)$ obeys Beer's law [Eq. (22)]; the absorption coefficient [Eq. (80)] has the coherent contribution

$$\alpha_{\text{coh}} = -\frac{\beta}{2} \frac{\alpha_0 \gamma \mathcal{D}_1 I_2 \mathcal{F}(\Delta) (\gamma \mathcal{D}_1 + 1)}{1 + I_2 \quad 1 + I_2 \mathcal{F}(\Delta) \gamma \mathcal{D}_1}, \quad (83)$$

where $\beta = 1 + \mathcal{E}_3^*/\mathcal{E}_1$. Hence $\beta = 0$ corresponds to $\mathcal{E}_1 = -\mathcal{E}_3^*$ (the FM case), in which case the population pulsations cancel, $\beta = 1$ corresponds to $\mathcal{E}_3^* = 0$ (a single-side-mode probe wave), and $\beta = 2$ gives $\mathcal{E}_1 = \mathcal{E}_3^*$ (the AM case), in which case the population pulsations from the beating of each side mode with the saturator add constructively.

6. COHERENT DIPS AND THE DYNAMIC STARK EFFECT

In this section we illustrate the probe-absorption coefficient for several different limiting conditions. First we consider the case of an upper-level lifetime long compared with the dipole lifetime. For a saturator wave tuned near the center of the absorption line, this case leads to a coherent dip in

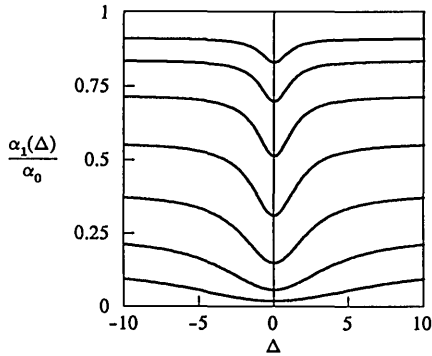


Fig. 6. Graphs of normalized probe-absorption coefficient of Eq. (84) for the single-probe case ($\beta = 1$) showing power-broadened Lorentzian coherent dips as saturator intensity is varied. The double-probe case has dips twice as deep. The medium is homogeneously broadened.

absorption versus probe detuning, caused by the inability of the population inversion to follow a probe-saturator beat frequency much larger than its decay rate. Hence the coherent contribution to the probe-absorption coefficient falls off as the beat frequency is increased. These dips allow one to measure the population-decay times, a fact particularly valuable for situations in which that decay is nonradiative, e.g., picosecond decays in liquids or semiconductors. We then consider the case of comparable population and dipole-decay times. We find that the coherent interaction leads to dynamic Stark splitting with resonances at the Rabi sidebands.

A. Short Dipole Lifetime Limit

We first treat the case in which the dipole lifetime T_2 ($\equiv 1/\gamma$) is much shorter than the upper-level lifetime $1/\gamma_a$. Then for beat frequencies $\Delta = \nu_2 - \nu_1$ small compared with the homogeneous linewidth, the \mathcal{D} 's in the absorption coefficient [Eq. (80)] reduce to $1/\gamma$. We then obtain from Eqs. (80) and (83) the single- and double-side-mode absorption coefficient

$$\alpha(\Delta) = \alpha_0 \left[\frac{1}{1 + I_2 \mathcal{L}_2} - \frac{\beta I_2 \mathcal{L}_2 \gamma_a^2}{\gamma_a^2 (1 + I_2 \mathcal{L}_2)^2 + \Delta^2} \right]. \quad (84)$$

The second term in Eq. (84) results from the population term d_1 in Eq. (78) and represents the attempt of the medium to follow the oscillating component in the coherent superposition of probe and saturator waves. Figure 6 illustrates Eq. (84) for the two-wave case. For the AM three-wave case, the dips are twice as deep, and the probes can actually experience gain owing to the coherent interaction with the medium.

We can understand the physical origin of the coherent dip as follows. The populations are effectively damped anharmonic oscillators with zero-resonance frequency that are driven by the product of the electric field and the induced polarization [see Eq. (32)]. This product includes an oscillating component at the frequency Δ . For Δ 's substantially less than the smaller population-difference bandwidth γ_a , the population differences pulsates, following the Δ component without phase lag. This response decreases the absorption, as one can see as follows. Because constructive interference between the probe and saturator waves (slightly larger total field intensity) produces above-average satura-

tion, that is, reduced absorption, and destructive interference yields reduced saturation, the average population response to the Δ component favors constructive interference, that is, it leads to increased probe transmission (reduced absorption). As Δ is increased beyond the smaller power-broadened level decay constant, the population difference pulsation lags behind, and the transmission is correspondingly reduced in a power-broadened Lorentzian fashion (typical of anharmonic oscillators). This reduction constitutes a decrease in the absorption versus Δ .

At first glance it might appear that the physics of nearly collinear interactions with infinite fringe spacing and of counterpropagating interactions are very different. However in both cases, the populations try to follow the probe-saturator beat-frequency component; their success is dependent on the ratio of the beat frequency to the level decay constants. In the counterpropagating case, the induced population pulsations are accompanied by spatial phase variations that produce the grating, allowing the saturator to scatter into the probe's path in spite of the difference in direction. In fact, as the angle between the probe and saturator waves is varied from the counterrunning ($\theta = 0$) to the corunning ($\theta = \pi/2$) case, a grating is induced that is perfectly phase matched to scatter the saturator wave into the path of the probe. Diffusion of the active atoms, such as in a gas, affects the copropagating and counterpropagating cases quite differently.

B. Comparable Population Difference and Dipole Lifetimes

Let us now consider the limit of Eqs. (80) and (83) in which the dipole response time T_2 is comparable with that of the populations (T_1). In this case both the dipole and population difference may not be able to follow the beat-frequency component. To understand the changes from Fig. 6, note that the equations of motion [Eqs. (28) and (32)] for the dipole and population difference form a coupled set of damped oscillators. When subjected to an oscillating component in the electric-dipole interaction energy, both dipoles and populations can introduce phase shifts for values of Δ comparable with or greater than the respective power-broadened bandwidths (the power-broadening factor times γ for the dipole and times γ_a for the population difference). The coupled dipole-population response to the probe-saturator beat frequency yields the coherent contribution [Eq. (80) or (83)] to the absorption coefficient α . In addition, α contains an incoherent (i.e., phase-independent) contribution α_{inc} resulting from the modification of population that is due to the saturator wave alone. For nonzero Δ , the sum of the dipole and population phase shifts can exceed $\pi/2$ and hence cause an increase in absorption ($\alpha_{\text{coh}} > 0$, whereas $\alpha_{\text{coh}} < 0$ in the dip region) relative to the α_{inc} value. This results in the shoulders in Figs. 7 and 8.

Figure 7 shows the $\gamma_a = 0.01\gamma$ and $\gamma_a = \gamma$ cases for a number of saturator intensities. Figure 7(a) reveals sharp power-broadened pulsation dips (produced by α_{coh}). Curves for the incoherent contribution α_{inc} are pure Lorentzians without the dips or increased shoulder area. In going from Fig. 7(a) to Fig. 7(b), we see the coherent dip change shape into a dynamic Stark splitting [$I_2 = 2$ in Fig. 7(b)], as two sidebands appear.

Figure 8 shows $\gamma_a = \gamma$ case with two sidebands, such as

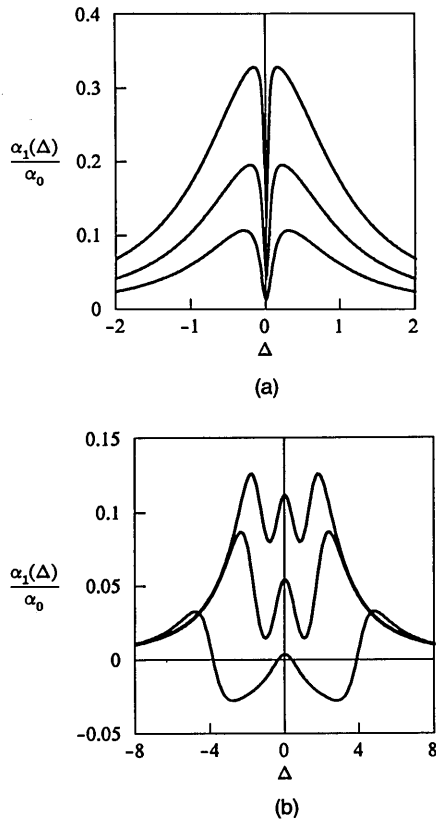


Fig. 7. Real part of the probe-absorption coefficient [Eq. (80)] versus probe-saturator detuning Δ for various saturator intensities and the decay-constant relationships: (a), $\gamma_a = 0.01 \gamma$; (b), $\gamma_a = \gamma$.

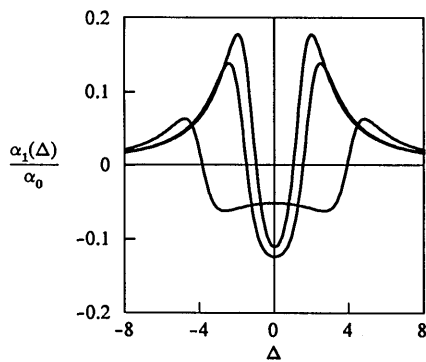


Fig. 8. Real part of the AM absorption coefficient versus Δ given by Eq. (80) with α_{coh} doubled and $\gamma_a = \gamma$. In comparison with Fig. 7(b), we see that the gain region is deeper when the probes work together.

occurs in AM spectroscopy. The coherent contribution is doubled, leading to a substantially larger gain region. The same kind of curve was published in the laser-instability discussions of Risken and Nummedal⁴⁶ and appears in the optical bistability instability of Bonifacio and Lugiato.⁴⁷ For those problems, side modes see gain given by curves like Fig. 8 (or the negative of these curves), and when that gain exceeds the cavity losses, the side modes build up. From the present discussion, it is apparent that these instabilities are due to the coherent contribution and hence to population pulsations.²⁷

Although the dip and Stark-splitting behaviors appear to be quite different from each other, plots of α_{coh} alone all

resemble the twin-peak, dip structure shown in Fig. 9. All the curves in Figs. 7 and 8 are obtained by adding the shoulder-dip structure in this figure to Lorentzians. Hence the dynamic Stark splitting is an extension of the coherent dip into regions of beat frequencies as large as or larger than the homogeneous linewidth.

The dynamic Stark effect can be interpreted in terms of an amplitude modulation of the dielectric polarization by optical nutation. In brief, the Bloch vector is transformed into a reference frame rotating at the frequency ν_2 , where it rotates because of a saturator-induced torque at the Rabi flopping frequency $\rho\mathcal{E}_2/\hbar$ and because of torque resulting from the probe-saturator beat frequency Δ . Resonance occurs for $\Delta = \rho\mathcal{E}_2/\hbar$, that is, the population pulsations interact resonantly with the Rabi flopping frequency.

This physics is illustrated by a simple analytic formula valid for the large I_2 shapes in Figs. 7(b) and 8. We have already seen from Eq. (55) that for the degenerate tuning, $\nu_1 = \nu_2$, the absorption coefficient saturates proportionally to $1/(1 + I_2\mathcal{L}_2)^2$. This saturation explains the small but positive bumps for $\Delta = 0$ in Figs. 7(b) and 8. Furthermore, for large I_2 and $\pm\Delta \approx \Omega = \rho\mathcal{E}_2/\hbar$, the absorption coefficient of Eq. (80) reduces to

$$\begin{aligned} \alpha_1(\Delta \approx \pm\Omega) &\approx -\frac{\alpha_2}{2} \frac{\gamma_a\gamma}{(\gamma_a + i\Delta)(\gamma + i\Delta) + \Omega^2} \\ &= -\frac{\alpha_2}{2} \frac{\gamma_a\gamma}{(\Omega + \Delta)(\Omega - \Delta) + i\Delta(\gamma_a + \gamma)/2} \\ &= \mp i \frac{\alpha_0}{4\Omega} \frac{\gamma_a\gamma}{(\gamma + \gamma_a)/2 \pm i(\Omega \pm \Delta)}. \end{aligned} \quad (85)$$

Note that this expression describes a symmetrically placed pair of indexlike curves for the absorption (real part) and Lorentzian curves for the index (imaginary part). The half-width of the Lorentzian is $(\gamma + \gamma_a)/2$, that is, the average of the dipole and population-difference decay constants, because the coherent term results from driving both the dipole and the populations at the frequency Δ . Similar features occur in the closely related phenomenon of resonance fluorescence, where fluorescence sidebands occur displaced by the Rabi flopping frequency on either side of the saturator frequency ν_2 . To obtain the AM double-side-mode absorption coefficient corresponding to Eq. (80), multiply expression (85) by 2.

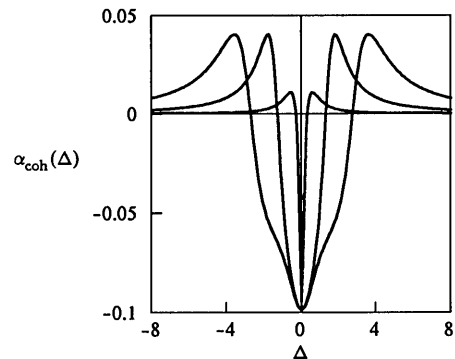


Fig. 9. α_{coh} versus probe-saturator beat frequency $\Delta = \nu_2 - \nu_1$ for a number of values of T_1/T_2 .

7. CONCLUSIONS

In this paper we have shown how the shifting of atomic energy levels as a result of the dynamic Stark effect can lead to new resonances in the nonlinear-optical susceptibility describing probe-wave absorption and four-wave mixing. This modification can equivalently be described as resulting from the new frequency components introduced into the temporal evolution of the induced dipole moment at the frequency of the population pulsations, which are driven by the beating of the various frequency components of the field. We have illustrated these points by treating a number of examples, all within a semiclassical context for one-photon two-level media.⁴⁸ Population pulsations and dynamic Stark effects play a key role in determining the nonlinear behavior of quantum systems interacting with quantized fields as well,⁴⁹ as has been described elsewhere.³³⁻³⁵

ACKNOWLEDGMENTS

R. W. Boyd is grateful for support through the U.S. Office of Naval Research grant N00014-86-K-0746. M. Sargent thanks the U.S. Office of Naval Research, the U.S. Army Research Office, and the U.S. Air Force Office of Scientific Research for funding support.

REFERENCES AND NOTES

1. N. Bloembergen and Y. R. Shen, *Phys. Rev. A* **133**, 37 (1964), gave the first expression for the probe-saturator absorption coefficient for arbitrary saturator intensity but omitted one of the two saturation terms in the population-pulsation contribution.
2. S. E. Schwartz and T. Y. Tan, *Appl. Phys. Lett.* **10**, 4 (1967), derived the single-side-mode coefficient valid to third order in the saturator-field amplitude.
3. E. V. Baklanov and V. P. Chebotaev, *Sov. Phys. JETP* **33**, 300 (1971); **34**, 490 (1972), derived the probe-absorption coefficient for corunning and counterunning waves in the Doppler-broadened limit for arbitrary saturator intensities.
4. S. Haroche and F. Hartmann, *Phys. Rev. A* **6**, 1280 (1972), derived the probe-absorption coefficient including Doppler broadening and some probe saturation for arbitrary saturator intensities.
5. B. R. Mollow, *Phys. Rev. A* **5**, 2217 (1972), derived the homogeneously broadened probe-absorption coefficient valid to all orders in the saturator intensity.
6. S. L. McCall, *Phys. Rev. A* **9**, 1515 (1974), derived the double-side-mode absorption coefficient in resonant media valid to all orders in the saturator intensity and including inhomogeneous broadening.
7. M. Sargent III, *Appl. Phys.* **9**, 127 (1976); M. Sargent III, P. E. Toschek, and H. G. Danielmeyer, *Appl. Phys.* **11**, 55 (1976), and M. Sargent III and P. E. Toschek, *Appl. Phys.* **11**, 107 (1976), investigated probe-saturator and modulation spectroscopy for a variety of decay, orientation, and inhomogeneous-broadening parameters for saturator waves of arbitrary intensity. This work is summarized in the review paper, Ref. 8.
8. M. Sargent III, *Phys. Rep. C* **43**, 223 (1978).
9. F. Y. Wu, S. Ezekiel, M. Ducloy, and B. R. Mollow, *Phys. Rev. Lett.* **38**, 1077 (1977), observed the gain in uninverted media predicted by the above theories.
10. For recent developments on probe-saturator spectroscopy, see G. Khitrova, P. Berman, and M. Sargent III, *J. Opt. Soc. B* **4**, 160 (1987).
11. G. Bjorklund, *Opt. Lett.* **5**, 15 (1980); M. Gehrtz, G. C. Bjorklund, and E. A. Whittaker, *J. Opt. Soc. Am. B* **2**, 1510 (1985).
12. R. W. P. Dreuer, J. L. Hall, F. W. Kowalski, J. Hough, G. M. Ford, A. G. Manley, and H. Wood, *Appl. Phys. B* **31**, 97 (1981).
13. L. W. Hillman, R. W. Boyd, J. Krasinski, and C. R. Stroud, Jr., *Opt. Commun.* **46**, 416 (1983).
14. M. S. Malcuit, R. W. Boyd, L. W. Hillman, J. Krasinski, and C. R. Stroud, Jr., *J. Opt. Soc. Am. B* **1**, 354 (1984).
15. D. A. Holm and M. Sargent III, *J. Opt. Soc. B* **3**, 732 (1986).
16. B. R. Mollow, *Phys. Rev.* **188**, 1969 (1969); *Phys. Rev. A* **7**, 1319 (1973); **5**, 2217 (1977).
17. F. Schuda, C. R. Stroud, Jr., and M. Hercher, *J. Phys. B* **7**, L198 (1974).
18. W. Hartig, W. Rasmussen, R. Schieder, and H. Walther, *Z. Phys. A* **278**, 205 (1978).
19. R. E. Grove, F. Y. Wu, and S. Ezekiel, *Phys. Rev. A* **15**, 227 (1977).
20. P. F. Liao, D. M. Bloom, and N. P. Economou, *Appl. Phys. Lett.* **32**, 813 (1978).
21. T. Fu and M. Sargent III, *Opt. Lett.* **4**, 366 (1979).
22. D. G. Steel and R. C. Lind, *Opt. Lett.* **6**, 587 (1981).
23. G. P. Agrawal, *Phys. Rev. A* **28**, 2286 (1983).
24. G. S. Agarwal, *Opt. Lett.* **8**, 566 (1983).
25. G. Grynberg, M. Pinard, and P. Verkerk, *Opt. Commun.* **50**, 261 (1984).
26. S. L. Le Boiteux, P. Simoneau, D. Bloch, F. A. M. De Oliveira, and M. Ducloy, *IEEE J. Quantum Electron.* **QE-22**, 1229 (1986).
27. The crucial role played by population pulsations in optical bistability and laser instabilities was first pointed out by S. T. Hendow and M. Sargent III, *Opt. Commun.* **40**, 385 (1982).
28. S. T. Hendow and M. Sargent III, *Opt. Commun.* **43**, 59 (1982).
29. S. T. Hendow and M. Sargent III, *J. Opt. Soc. Am. B* **2**, 84 (1985) and other papers in this special issue on optical instabilities.
30. L. W. Hillman, R. W. Boyd, and C. R. Stroud, Jr., *Opt. Lett.* **7**, 426 (1982).
31. M. L. Minden and L. W. Casperson, *J. Opt. Soc. Am. B* **2**, 120 (1985).
32. R. W. Boyd, M. G. Raymer, and L. M. Narducci, eds., *Optical Instabilities* (Cambridge U. Press, Cambridge, 1986).
33. The first degenerate or nondegenerate quantum theory of four-wave mixing and of optical instabilities was given by M. Sargent III, M. S. Zubairy, and F. deMartini, *Opt. Lett.* **8**, 76 (1983). Detailed derivations are given in M. Sargent III, D. A. Holm, and M. S. Zubairy, *Phys. Rev. A* **31**, 3112 (1985); S. Stenholm, D. A. Holm, and M. Sargent III, *Phys. Rev. A* **31**, 3124 (1985).
34. M. D. Reid and D. F. Walls, *Phys. Rev. A* **31**, 1622 (1985); **33**, 4465 (1986); **34**, 4929 (1986).
35. D. A. Holm and M. Sargent III, *Phys. Rev. A* **35**, 2150 (1987).
36. S. H. Autler and C. H. Townes, *Phys. Rev.* **100**, 703 (1955).
37. C. Cohen-Tanoudji and S. Reynaud, *J. Phys. B* **10**, 345 (1977); **10**, 365 (1977); **10**, 3211 (1977).
38. E. Courtens and A. Szöke, *Phys. Rev. A* **15**, 1588 (1977); **17**, 2 (1978).
39. P. L. Knight and P. W. Milonni, *Phys. Rep.* **66**, 21 (1980). This review paper contains an extensive reference list.
40. W. E. Lamb, Jr., *Phys. Rev. A* **134**, 1429 (1964).
41. M. Sargent III, M. O. Scully, and W. E. Lamb, Jr., in *Laser Physics* (Addison-Wesley, Reading, Mass., 1974).
42. I. I. Rabi, *Phys. Rev.* **51**, 652 (1937).
43. D. J. Harter, P. Narum, M. G. Raymer, and R. W. Boyd, *Phys. Rev. Lett.* **46**, 1192 (1981).
44. D. J. Harter and R. W. Boyd, *Phys. Rev. A* **29**, 739 (1984).
45. R. W. Boyd, M. G. Raymer, P. Narum, and D. J. Harter, *Phys. Rev. A* **24**, 411 (1981).
46. H. Risken and K. Nummedal, *J. Appl. Phys.* **39**, 4662 (1968).
47. R. Bonifacio and L. A. Lugiato, *Lett. Nuovo Cimento* **21**, 505 (1978).
48. A similar treatment for two-photon, two-level media has been given by M. Sargent III, S. Ovadia, and M. S. Lu, *Phys. Rev. A* **32**, 1596 (1985).
49. H. J. Carmichael and D. F. Walls, *J. Phys. B* **9**, 1199 (1976).

Robert W. Boyd



Robert W. Boyd received the B.S. degree in physics in 1969 from the Massachusetts Institute of Technology and the Ph.D. degree in physics in 1977 from the University of California, Berkeley. His thesis work involved the use of nonlinear optical techniques for infrared detection for astronomy. In 1977 he became an assistant professor and in 1982 became an associate professor at The Institute of Optics, University of Rochester, Rochester, New York. His research interests include studies of the nonlinear optical

properties of materials, nonlinear optical interactions involving atomic Rydberg states, and the development of new laser systems.